DFT Calculations of Proton Hyperfine Coupling Constants for $[VO(H_2O)_5]^{2+}$: Comparison with Proton ENDOR Data

Sarah C. Larsen†

Department of Chemistry, University of Iowa, Iowa City, Iowa 52242

Received: April 26, 2001; In Final Form: June 7, 2001

Density functional theory (DFT) methods, as implemented in the Amsterdam Density Functional Theory (ADF) program, were used to calculate the proton hyperfine coupling constants for $[VO(H_2O)_5]^{2+}$. Qualitative agreement between the calculated and experimental proton hyperfine coupling constants for the axial water molecule in $[VO(H_2O)_5]^{2+}$ was observed. For the equatorial water molecules, the proton hyperfine coupling constants depend on the orientation of the water molecule relative to the equatorial plane. DFT calculations revealed that the isotropic component of the proton hyperfine coupling constant for an equatorial water molecule has a trigonometric dependence on β, where β is the OVOH dihedral angle. The relative sizes of the isotropic hyperfine coupling constants for two protons on one water molecule can be used to determine the orientation of the water molecule with respect to the equatorial plane. The computational results were compared with experimental single-crystal and powder ENDOR data from the literature (Atherton, N. M.; Shackleton, J. F. *Mol. Phys.* **1980**, *39*, 1471).[1]

Introduction

Electron paramagnetic resonance (EPR) techniques are widely used to study paramagnetic transition metal complexes.[2,3] The EPR parameters, the electronic **g** factor, and the electron nuclear hyperfine coupling constant (**A**) are determined from the experimental EPR spectrum and provide information about the electronic environment of the paramagnetic center. The interpretation of the experimental EPR parameters often relies on empirical trends[4] and could be significantly enhanced by the application of computational methods for the calculation of EPR parameters. Recently, density functional theory (DFT) methods for the calculation of EPR parameters (**g** and **A** tensors) for transition metal complexes were introduced by several groups.[5−13] The main advantage of DFT methods compared to traditional ab initio methods[14−16] is that they are computationally less expensive. In addition, DFT methods have been used successfully to calculate other properties of transition metal complexes.[17,18] The number of systems that the DFT methods has been applied to for the calculation of EPR parameters has been rather limited, and therefore, the validity of using these methods for the interpretation of experimental EPR data is largely untested.

We reported a study[19] in which the EPR parameters for VO^{2+} model complexes were calculated using the commercial Amsterdam Density Functional Theory (ADF) program,[20−22] which implements the methods of Van Lenthe[11−13] for **g** and **A** tensor calculations. The computational results were then used to interpret the EPR data for VO^{2+}-exchanged zeolites. The calculated **g** values were in very good agreement with the experimental values, but the **A** (vanadium) values were systematically too low by approximately 25%. Importantly, these DFT calculations were able to reproduce the empirical trends in **g** and **A** with ligand identity despite the systematic deviation of the **A** values. Munzarova and Kaupp attributed the deviations in calculated **A** values for similar transition metal complexes to spin polarization and spin contamination effects which are not adequately treated by the DFT methods.[9,10]

Using modern EPR techniques, such as ENDOR (electron nuclear double resonance) and ESEEM (electron spin−echo envelope modulation), ligand hyperfine coupling constants that are too small to be resolved in traditional continuous wave (CW) EPR experiments (due to large line widths) can be observed. ESEEM and ENDOR have been widely used in studies of VO^{2+} complexes to measure the hyperfine coupling constants of nitrogen and water ligands.[4,23−34] Few theoretical calculations of ligand hyperfine coupling constants for transition metal complexes have been reported in the literature.[10,12,16]

The objective of this study is to demonstrate that DFT methods can be successfully used to calculate the proton hyperfine coupling constants for $[VO(H_2O)_5]^{2+}$. We have chosen $[VO(H_2O)_5]^{2+}$ as the focus of this study because single-crystal ENDOR data[1] are available for comparison with the calculated values. The proton hyperfine coupling constants for the water molecules will be calculated using the DFT methods implemented in the ADF program. The effect of the orientation of the water molecules with respect to the V═O bond on the isotropic proton hyperfine coupling constant (A_{iso}) will be examined. The validity of this computational approach for interpreting ENDOR data will be assessed.

Computational Details

Geometry optimization of $[VO(H_2O)_5]^{2+}$ was performed using the Amsterdam Density Functional (ADF) program package.[20−22] The program implements numerical integration in Cartesian space,[35] and gradients for geometry optimizations are solved analytically.[36,37] The equations and methods for calculation of **g** tensors and **A** tensors are due to van Lenthe et al.[11,12,38] The basis set designated *V* in the ADF program was used for V, C, O, and H, in geometry optimizations, **g** tensor calculations, and **A** tensor calculations. Basis set *V* is a triple-ζ basis of Slater-type orbitals with two polarization functions for H−Ar. In general, all electron calculations were performed with no frozen cores on the atoms of the molecule.[39]

Relativistic effects were included in all calculations using the zero order relativistic approximation (ZORA).[40−44] Two methods

† Fax: (319) 335-1270. E-mail: sarah-larsen@uiowa.eu.

10.1021/jp0116003 CCC: $20.00
Published on Web 08/15/2001

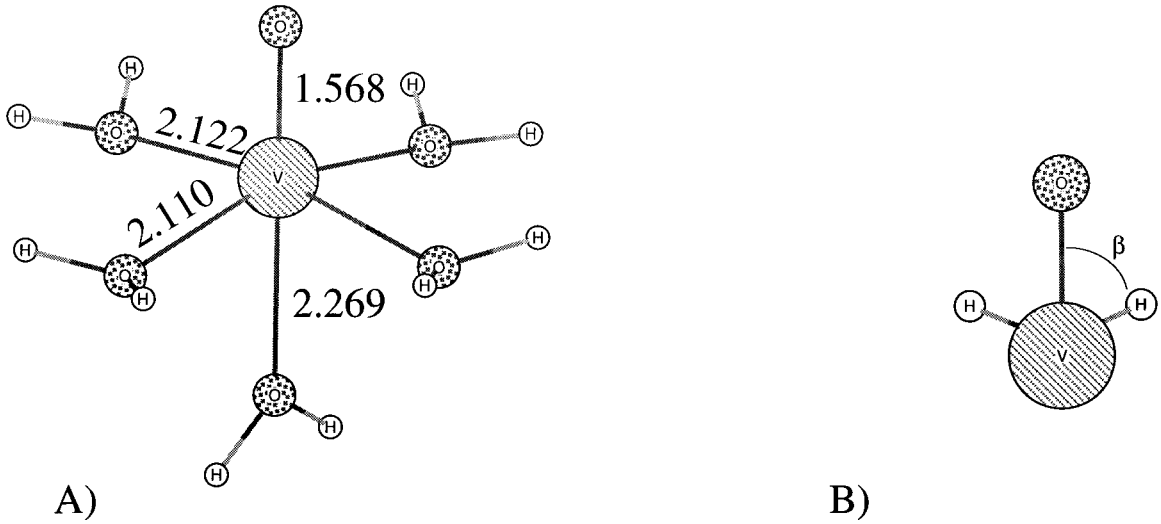

Figure 1. Optimized geometry for (A) $[VO(H_2O)_5]^{2+}$. Bond lengths are given in angstroms. The dihedral angle, β, is defined in (B) from the perspective of looking down the V−O equatorial bond.

TABLE 1: Selected Geometrical Parameters of $[VO(H_2O)_5]^{2+}$ and Comparison with Experimental Values

molecule	sym	$R_{V=O}$,[a] Å	R_{V-L},[b] Å	$\angle_{O\approx VL}$[c]	β(OVOH)[d]	source
$[VO(H_2O)_5]^{2+}$	C_{2v}	1.568	2.110, 2.122 2.269 (axial)	99.5, 96.3	−69.5, 69.5 68.7, −68.7	DFT calc[19]
$VOSO_4 \cdot 5H_2O$		1.591	2.048, 1.983 (SO_4) 2.223 (axial)	99.6, 97.9, 93.8, 100.7 (SO_4)		expt[e]

[a] $R_{V=O}$ is the vanadyl bond distance. [b] R_{V-L} is the bond distance between the vanadium ion and the ligand atoms. L refers to equatorial ligands unless labeled otherwise. [c] $\angle_{O=V-L}$ is the bond angle between the vanadium ion and the equatorial ligand atoms. [d] β is defined as the dihedral angle OVOH. See Figure 1B. [e] From the crystal structure for $VOSO_4 \cdot 5H_2O$ from ref 48.

of including the relativistic effects were utilized. Scalar relativistic effects were employed for geometry optimizations and **A** tensor calculations. Spin−orbit relativistic effects were employed for **g** tensor calculations. The relativistic atomic potentials necessary for the relativistic calculations for each atom were calculated using the auxiliary program DIRAC, which is supplied with the ADF program package. The density functional for all calculations used the VWN[45] local density approximation and the generalized gradient approximation, with the exchange correction of Becke[46] and the correlation correction of Perdew.[47] Each molecule studied contained one unpaired electron; therefore geometry optimizations and **A** tensor calculations were performed spin-unrestricted while restrictions due to the **g** tensor calculation method required these calculations to be performed spin-restricted.

Results

Geometry Optimization. The results of the geometry optimization for $[VO(H_2O)_5]^{2+}$ are presented in Figure 1A and Table 1. $[VO(H_2O)_5]^{2+}$ was restricted to C_{2v} symmetry such that the four equatorial water molecules were located in the equatorial plane (Figure 1A).[19] The resulting V═O bond length was 1.568 Å with equatorial V−O bond lengths of 2.122 and 2.110 Å.[19] The axial V−O bond length was 2.269 Å. This structure served as the starting point for calculations in which one of the water molecules was systematically rotated to vary the dihedral angle, β (shown in Figure 1B), in order to quantify the effect of the orientation of the water molecule on the proton hyperfine coupling constant. The geometrical parameters obtained from the crystal structure for $VOSO_4 \cdot 5H_2O$[48] are listed in Table 1 for comparison with the optimized structures. The calculated V═O and V−O bond lengths for $[VO(H_2O)_5]^{2+}$ deviate by 0.04−0.07 Å relative to the bond lengths from the crystal structure of $VOSO_4 \cdot 5H_2O$. The size of the deviations between the experimental and the calculated bond lengths are similar to those reported by Patchkovski and Ziegler for DFT geometry optimizations of d^1 MEX_4 transition metal complexes.[5]

TABLE 2: Comparison of Calculated and Experimental Proton Hyperfine Coupling Constants for the Axial Water in $[VO(H_2O)_5]^{2+}$ Determined from Single-Crystal ENDOR Data

A_{iso}/MHz	$A_{D,i}$[a]/MHz	reference
0.10[b]	−3.13, −3.01, 6.16	DFT (Figure 1A), this work
0.04[c]	−3.40, −3.10, 6.51	single-crystal ENDOR[1]
0.01	−3.37, −3.19, 6.56	single-crystal ENDOR[1]
0.3[b]	−3.0, −3.0, 6.0	powder ENDOR[25]

[a] $A_{D,i}$, where $i = x, y, z$. [b] The two protons (H_a and H_b) on the axial water molecule are equivalent. [c] The two protons (H_a and H_b) on the axial water molecule are not equivalent

DFT Calculations of Vanadium EPR Parameters. Using the geometry-optimized structure of the vanadyl $[VO(H_2O)_5]^{2+}$ with all of the water molecules approximately in the equatorial plane (Figure 1A), the **g** and **A** tensors for vanadium were calculated using the ADF program and the methods of van Lenthe.[11,12] The results have been reported previously for the structure in Figure 1A.[19] The **g** values calculated for $[VO(H_2O)_5]^{2+}$ ($g_{||} = 1.930$, $g_{\perp} = 1.986$) deviate by 3−8 ppt (parts per thousand) from the experimental values for $[VO(H_2O)_5]^{2+}$ ($g_{||} = 1.933$, $g_{\perp} = 1.978$[4] and $g_{||} = 1.936$, $g_{\perp} = 1.982$[49]). The **A** values calculated for $[VO(H_2O)_5]^{2+}$ ($A_{||} = 408$, $A_{\perp} = 148$ MHz) are systematically too low by approximately 25% when compared to the experimental values for $[VO(H_2O)_5]^{2+}$ ($A_{||} = 547$, $A_{\perp} = 212$;[4] $A_{||} = 534$, $A_{\perp} = 210$;[49] and $A_{||} = 547$, $A_{\perp} = 208.5$ MHz[18]).

Proton Hyperfine Coupling Constants for the Axial Water Molecule. The calculated proton hyperfine coupling constants for the axial water molecule in $[VO(H_2O)_5]^{2+}$ (Figure 1A) are listed in Table 2. For comparison, the experimental proton hyperfine coupling constants for $[VO(H_2O)_5]^{2+}$ measured by single-crystal[1,50] and powder ENDOR spectroscopy[25] are also

given in Table 2. The calculated hyperfine coupling constants qualitatively reproduce the experimental values.

Two interactions contribute to the observed hyperfine coupling constant (A_i): an isotropic or Fermi contact interaction and an anisotropic or dipolar interaction. The isotropic hyperfine coupling constant for a nucleus, n, $A_{iso}(n)$, is defined by[2]

$$A_{iso}(n) = A_{FC} = \frac{4\pi}{3}\beta_e\beta_n g_e g_n \langle S_z\rangle \rho_n^{\alpha-\beta} \qquad (1)$$

where

$$A_{FC} = \text{Fermi contact term}$$

$$\rho_n^{\alpha-\beta} = \text{spin density at position of nucleus}$$

$$\langle S_z\rangle = \text{expectation value of } z \text{ component of the electron spin}$$

In eq 1, g_e and g_n (and β_e and β_n) refer to the electronic and nuclear g factors (electronic and nuclear Bohr magnetons), respectively. Using the point-dipole approximation in the strong field limit, the dipolar hyperfine coupling constant, $A_{D,i}$, is given by[28]

$$A_{D,i} = \frac{g_e|\beta_e|g_n|\beta_n|(3\cos^2\phi - 1)}{r^3};\ i = x, y, z \qquad (2)$$

The modulus, r, is defined as the position vector, r, between the proton and the electron and ϕ is the angle between r and H_0, the applied magnetic field.

The calculated isotropic component of the hyperfine coupling constant for the protons of the axial water molecule is ~ -0.1 MHz (DFT), compared to experimental ENDOR values ranging from -0.3 to 0.01 MHz. The small value of the isotropic hyperfine coupling constant is due to fact that the molecular orbitals of the protons of the axial water molecule do not overlap with the vanadium d_{xy} orbital, which contains the unpaired electron.[51] Therefore, the spin density at the protons in the axial water ligand is very small.[1,25,52,53] The dipolar hyperfine coupling constants can be used to calculate distances using eq 2. Atherton and Shackleton used the point-dipole approximation and the dipolar hyperfine coupling constants to determine the positions of the protons in $[VO(H_2O)_5]^{2+}$ in $Mg(NH_4)_2(SO_4)_2\cdot 6H_2O$ single crystals.[1,50]

Proton Hyperfine Coupling Constants for Equatorial Water Molecules. To understand how the proton hyperfine coupling constants in $[VO(H_2O)_5]^{2+}$ vary with the orientation of an equatorially ligated water molecule, one equatorial water ligand was systematically rotated by 15° increments and the proton hyperfine coupling constants were calculated at each position. The other water molecules remained stationary. The starting point was the geometry-optimized structure of $[VO(H_2O)_5]^{2+}$ (Figure 1A) with all of the water molecules located in the equatorial plane. After each rotation, the EPR parameters for the $[VO(H_2O)_5]^{2+}$ were calculated using the DFT methods in the ADF program. The calculated proton hyperfine coupling constants are listed in Table 3. The angle of rotation of the water molecule as well as the dihedral angles (defined in Figure 1B) for each of the protons (H_a and H_b) are listed in Table 3. H_a and H_b refer to the two protons on a single water molecule. The isotropic hyperfine coupling constants (A_{iso}) for each proton in the rotated water molecule and the dipolar portion ($A_{D,i}$) of the hyperfine coupling tensor are listed in Table 3.

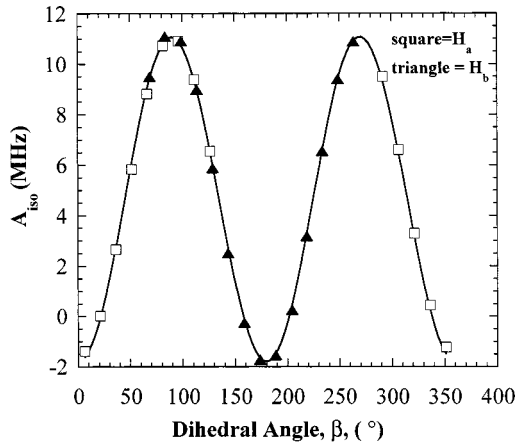

Figure 2. Graph showing the variation of the calculated value of A_{iso} as a function of the dihedral angle, β, for the two protons, H_a (□) and H_b (▲), in an equatorial water molecule in $[VO(H_2O)_5]^{2+}$. The water molecule was rotated 180° from the initial orientation shown in Figure 1A. The data were fit to the functional form $A_{iso} = A + B\cos^2\beta$, where A and B are equal to 11.07 and -12.86 MHz, respectively.[54] Data taken from Table 3.

The calculated isotropic proton hyperfine coupling constants (A_{iso}) for protons, H_a and H_b, as a function of dihedral angle are plotted in Figure 2. A_{iso} varies periodically and can be fit to the following functional form:

$$A_{iso} = A + B\cos^2\beta \qquad (3)$$

where A_{iso} is the isotropic component of the proton hyperfine coupling constant, A and B are constants, and β is the dihedral angle. Regression of the data in Figure 2 yields the constants A and B which are equal to 11.07 and -12.86 MHz, respectively.[54] This provides a quantitative expression for the relationship between A_{iso} and the dihedral angle, β. A similar expression has been used previously by Dikanov and co-workers in ESEEM studies of VO^{2+} complexes.[53] In their case, the angle, β, was defined as the angle of rotation of the water molecule relative to the equatorial plane of the complex. Similar empirical expressions have been used to describe the interaction of an unpaired electron in a π orbital of a hydrocarbon with the C−H bond on the β-carbon.[2,55] This expression has been widely used and has been interpreted as a hyperconjugation effect of the unpaired electron.

In this case, the interaction involves the unpaired electron in the vanadium d_{xy} orbital[51] and the molecular orbitals on the hydrogen atoms of the water molecule. As would be qualitatively expected, the size of A_{iso} for the water protons is largest when the water molecule is close to the equatorial plane and overlap with the hydrogen molecular orbitals is maximized. A_{iso} becomes smaller as the protons of the water molecule are rotated out of the equatorial plane and overlap with the proton molecular orbitals is negligible. This trend is clearly observed in the data plotted in Figure 2. As the dihedral angle approaches 0°, A_{iso} also approaches 0. As the dihedral angle approaches 90°, A_{iso} reaches a maximum value. This behavior has been discussed previously in the context of explaining experimental ENDOR and ESEEM data.[1,25,50,52,53]

Discussion

Interpretation of Single-Crystal ENDOR Data Using the Computational Results. The single-crystal proton ENDOR results[1] for the equatorial water ligands of $[VO(H_2O)_5]^{2+}$ in $Mg(NH_4)_2(SO_4)_2\cdot 6H_2O$ single crystals are given in Table 4. A_{iso}

TABLE 3: Calculated Proton Hyperfine Coupling Constants for an Equatorial Water Molecule (H_a-O-H_b) of $[VO(H_2O)_5]^{2+}$

	H_a			H_b		
$\angle_{rotation}$[a]	β[b]	A_{iso}/MHz	$A_{D,i}$[c]/MHz	β[b]	A_{iso}/MHz	$A_{D,i}$[c]/MHz
0	68.74	9.49	−4.30, −4.03, 8.32	291.26	9.49	−4.30, −4.03, 8.32
15	83.74	11.1	−4.46, −4.00, 8.48	306.23	6.6	−4.17, −4.01, 8.18
30	98.78	10.92	−4.57, −3.99, 8.56	321.21	3.29	−4.24, −3.84, 8.08
45	113.7	8.98	−4.56, − 4.05, 8.62	336.3	0.45	−4.41, −3.66, 8.07
60	128.7	5.89	−4.51, −4.10, 8.59	351.26	−1.23	−4.63, −3.54, 8.16
75	143.7	2.52	−4.49, −4.00, 8.51	6.25	−1.38	−4.80, −3.53, 8.34
90	158.74	−0.25	−4.52, −3.83, 8.36	21.26	0.02	−4.84, −3.68, 8.53
105	173.74	−1.72	−4.51, −3.67, 8.18	36.26	2.66	−4.73, −3.94, 8.66
120	188.74	−1.54	−4.54, −3.56, 8.04	51.25	5.84	−4.51, −4.22, 8.73
135	204.74	0.25	−4.42, −3.55, 7.97	66.26	8.81	−4.46, −4.23, 8.70
150	218.74	3.19	−4.35, −3.65, 8.02	81.25	10.72	−4.52, −4.07, 8.61
165	233.74	6.56	−4.27, −3.87, 8.14	96.26	10.92	−4.44, −4.03, 8.47
180	248.74	9.40	−4.28, −4.04, 8.31	111.25	9.39	−4.27, −4.05, 8.32
195	263.7	10.89	−4.45, −4.03, 8.47	126.3	6.55	−4.28, −3.88, 8.14

[a] $\angle_{rotation}$ is defined as the angle of rotation of an equatorial water molecule around the V−O equatorial bond in $VO(H_2O)_5^{2+}$. The starting structure is the geometry-optimized structure for $[VO(H_2O)_5]^{2+}$ (Figure 1A). Each water molecule was rotated by $\angle_{rotation}$. [b] β is defined as the dihedral angle OVOH. See Figure 1B. [c] $A_{D,i}$, where $i = x, y, z$.

TABLE 4: Proton Hyperfine Coupling Constants for Equatorial Water Molecules in $[VO(H_2O)_5]^{2+}$ Determined from Single-Crystal ENDOR Data[1]

proton no.[a]	A_{iso}/MHz	$A_{D,i}$[b]/MHz
17	−0.39	−4.41, −3.97, 8.38
18	4.08	−5.26, −4.32, 9.58
17′	−0.05	−4.69, −4.41, 9.11
18′	4.57	−4.91, −4.10, 9.01
19	8.67	−4.75, −4.45, 9.20
20	7.14	−4.94, −4.31, 9.25
19′	7.73	−5.12, −4.64, 9.76
20′	6.96	−5.13, −4.75, 9.88

[a] Numbering scheme from ENDOR work of Atherton and Shackleton was used.[1] [b] $A_{D,i}$, where $i = x, y, z$.

and the dipolar components of the hyperfine coupling tensor ($A_{D,i}$) are listed. The analysis of the ENDOR data led Atherton and Shackleton to conclude that two water molecules (protons 19, 20, 19′, 20′) were oriented approximately in the equatorial plane while the other two water molecules (protons 17, 18, 17′, 18′) were located approximately perpendicular to the equatorial plane.[1] The dipolar approximation was the basis for their analysis.[1,50]

To facilitate a comparison of the single-crystal ENDOR data and the calculated proton hyperfine coupling constants, A_{iso} versus the angle of rotation of the water molecule from the initial configuration was graphed as shown in Figure 3 using the data from Table 3. The data in Figure 3 illustrate that A_{iso} for H_a and H_b are initially equivalent. The two curves for H_a and H_b then diverge and eventually cross again when the angle of rotation of the water molecule is equal to 90° and then 180°. Using the data in Figure 3 to interpret the single-crystal ENDOR data in Table 4, we conclude that protons 19, 20 and 19′, 20′ are located approximately in the equatorial plane. This conclusion is based on the following two observations: (1) the A_{iso} values for the two protons on each water molecule are approximately equivalent, indicating that the angle of rotation of the water molecule is either 0°, 90°, or 180°; (2) A_{iso} is large (ranging from 6.96 to 8.67 MHz), indicating substantial overlap between the vanadium d_{xy} orbital and the proton molecular orbitals and ruling out the 90° rotation angle. Protons 17, 18 and 17′, 18′ clearly have a different orientation than protons 19, 20, and 19′, 20′ since the A_{iso} values are quite different for each proton on the water molecule. Protons H_a and H_b have A_{iso} values of ∼0 and ∼4 MHz, respectively, for protons 17, 18 and 17′, 18′. This allows us to put bounds of ∼70°−115°

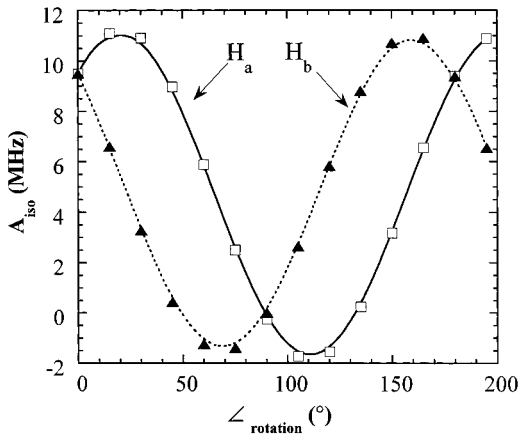

Figure 3. Proton hyperfine coupling constant, A_{iso}, plotted versus the angle of rotation of an equatorial water molecule in $[VO(H_2O)_5]^{2+}$ relative to the equatorial plane. The water molecule was rotated 180° from the initial orientation shown in Figure 1A. The variation of A_{iso} for each proton, H_a (□) and H_b (▲), is shown as a function of the rotation angle. Data taken from Table 3.

on the orientation of the other two equatorial water molecules (17, 18 and 17′, 18′). These results are consistent with the conclusions of Atherton and Shackelton which were based primarily on an analysis of the dipolar hyperfine coupling constants.[1,50]

Validity of DFT Calculations for Interpreting ENDOR Data. The DFT calculations of the proton hyperfine coupling constants for $[VO(H_2O)_5]^{2+}$ reproduce the qualitative features of the experimental ENDOR data. The calculated hyperfine coupling constants for the protons on the axial water molecule qualitatively agree with the experimentally observed hyperfine coupling constants. The calculated hyperfine coupling constants for the protons on the equatorial water molecules depend on the orientation of the water molecule with respect to the equatorial plane. By comparing the relative values of A_{iso} values for the two protons on the water molecule, one can ascertain the approximate orientation of the equatorial water molecule. When the water molecule is located in or nearly in the equatorial plane, A_{iso} for the two protons on the water molecule are equivalent and at a maximum as shown in Figure 3. When the water molecule is rotated 90° out of the plane, A_{iso} for the two protons is again equal, but the value is nearly at the minimum as shown in Figure 3. The principle values of the proton hyperfine coupling constant tensor, A_i, exhibit the same orienta-

tion dependence as the isotropic hyperfine coupling constants. Therefore, a similar analysis can be developed if only one of more of the principal values of the proton hyperfine tensor is experimentally measured.

Since the relative sizes of the two proton hyperfine coupling constants for a single water molecule provide insight into the orientation of the water molecule, the absolute accuracy of the calculated values is not essential to this analysis. For example, the proton hyperfine coupling constants will also depend on the distance of the vanadium atom from the equatorial plane containing the water molecules. However, the qualitative features of the orientation dependence of the hyperfine coupling constants are not expected to change as the distance of the vanadium atom from the equatorial plane is varied.

One aspect of these calculations that has not yet been discussed is that the calculations are for gas phase complexes and do not include any environmental effects. Malkina and coworkers have suggested that an agreement of 10−15% should be expected when comparing calculated (gas phase) and experimental (condensed phase) EPR hyperfine coupling constants.[9,10] Previous studies have indicated that the structure of $[VO(H_2O)_5]^{2+}$ is similar in frozen aqueous solution and in single crystals.[52] It was suggested that internal hydrogen bonding forces played an important role in determining the geometry of $[VO(H_2O)_5]^{2+}$.[52] In light of this, the role of the environment is not likely to be crucial to the calculations reported here. However, for other systems, it may be important to include environmental effects.[16]

The results of this study demonstrate that DFT calculations of ligand hyperfine coupling constants for VO^{2+} systems can be used to enhance the interpretation of experimental ENDOR data. The DFT calculations provide insight into the orientation dependence of the proton hyperfine coupling constants and, therefore, into the structure of $[VO(H_2O)_5]^{2+}$. Future studies will focus on DFT calculations of hyperfine coupling constants for VO^{2+} complexes with nitrogen ligands and may have important implications for the interpretation of ESEEM and ENDOR data for many biological systems.[32,33,56−60]

Conclusions

DFT methods implemented in the ADF program were used to calculate the proton hyperfine coupling constants for $[VO(H_2O)_5]^{2+}$. The calculated proton hyperfine coupling constants were compared with the results of an experimental single-crystal proton ENDOR study of $[VO(H_2O)_5]^{2+}$ in $Mg(NH_4)_2(SO_4)_2 \cdot 6H_2O$.[1] The calculated isotropic hyperfine coupling constant for the protons of the axial water molecule was approximately −0.1 MHz, compared to −0.04 and 0.1 MHz for the experimentally observed values. The isotropic hyperfine coupling constants of the equatorial water molecules depend on the orientation of the water molecules relative to the vanadyl bond. DFT calculations were used to explicitly map the orientation dependence of the isotropic hyperfine coupling constants. The relative sizes of the isotropic hyperfine constants for the two protons of an equatorial water molecule were used to determine the orientation of the water molecule with respect to the equatorial plane. Overall, the calculations can be used to analyze experimental ENDOR data and to demonstrate the validity of using DFT methods to enhance the interpretation of ESEEM and ENDOR data of vanadyl complexes.

Acknowledgment. S.C.L. gratefully acknowledges the support of NSF (CTS-99-73431) and Jan Jensen and Russell Larsen for helpful discussions.

Supporting Information Available: The optimized Cartesian coordinates for $[VO(H_2O)_5]^{2+}$ are given in Table S1. This material is available free of charge via the Internet at http://pubs.acs.org.

References and Notes

(1) Atherton, N. M.; Shackleton, J. F. *Mol. Phys.* **1980**, *39*, 1471.
(2) Weil, J. A.; Bolton, J. R.; Wertz, J. E. *Electron Paramagnetic Resonance: Elementary Theory and Practical Applications*; John Wiley & Sons: New York, 1994.
(3) Weltner, W., Jr. *Magnetic Atoms and Molecules*; Dover Publications: Mineola, NY, 1983.
(4) Chasteen, N. D. In *Biological Magnetic Resonance*; Berliner, L. J., Reuben, J., Eds.; Plenum: New York, 1981; Vol. 3; p 53.
(5) Patchkovskii, S.; Ziegler, T. *J. Chem. Phys.* **1999**, *111*, 5730.
(6) Schreckenbach, G.; Ziegler, T. *J. Phys. Chem. A* **1997**, *101*, 3388.
(7) Patchkovskii, S.; Ziegler, T. *J. Am. Chem. Soc.* **2000**, *122*, 3506.
(8) Malkina, O. L.; Vaara, J.; Schimmelpfennig, B.; Munzarova, M.; Malkin, V. G.; Kaupp, M. *J. Am. Chem. Soc.* **2000**, *122*, 9206.
(9) Munzarova, M.; Kaupp, M. *J. Phys. Chem. A* **1999**, *103*, 9966.
(10) Munzarova, M. L.; Kubacek, P.; Kaupp, M. *J. Am. Chem. Soc.* **2000**, *122*, 11900.
(11) van Lenthe, E.; Wormer, P. E. S.; van der Avoird, A. *J. Chem. Phys.* **1997**, *107*, 2488.
(12) van Lenthe, E.; van der Avoird, A.; Wormer, P. E. S. *J. Chem. Phys.* **1998**, *108*, 4783.
(13) van Lenthe, E.; van der Avoird, A.; Hagen, W. R.; Reijerse, E. J. *J. Phys. Chem. A* **2000**, *104*, 2070.
(14) Mattar, S. M.; Doleman, B. J. *Chem. Phys. Lett.* **1993**, *216*, 369.
(15) Knight, L. B., Jr.; Babb, R.; Ray, M.; Banisaukas, T. J., III; Russon, L.; Dailey, R. S.; Davidson, E. R. *J. Chem. Phys.* **1996**, *105*, 10237.
(16) Leitão, A. A.; Coelho Neto, J. A.; Pinhal, N. M.; Bielschowsky, C. E.; Vugman, N. V. *J. Phys. Chem. A* **2001**, *105*, 614.
(17) Ziegler, T. *Chem. Rev.* **1991**, *91*, 651.
(18) Grant, C. V.; Cope, W.; Ball, J. A.; Maresch, G. G.; Gaffney, B. J.; Fink, W.; Britt, R. D. *J. Phys. Chem. B* **1999**, *103*, 10627.
(19) Carl, P. J.; Isley, S. L.; Larsen, S. C. *J. Phys. Chem. A* **2001**, *105*, 4563.
(20) ADF, http://tc.chem.vu.nl/SCM; Department of Theoretical Chemistry, Vrije Universiteit, Amsterdam, 1999.
(21) Baerends, E. J.; Ellis, D. E.; Ros, P. *Chem. Phys.* **1973**, *2*, 41.
(22) *Methods and Techniques in Computational Chemistry METECC-95*; Guerra, F. C., Visser, O., Snijders, J. G., Velde, G. T., Baerends, E. J., Eds.; STEF: Cagliari, 1995; p 305.
(23) Mulks, C. F.; van Willigen, H. *J. Phys. Chem.* **1981**, *85*, 1220.
(24) Mulks, C. F.; Kirste, B.; van Willigen, H. *J. Am. Chem. Soc.* **1982**, *104*, 5906.
(25) van Willigen, H. *J. Magn. Reson.* **1980**, *39*, 37.
(26) van Willigen, H.; Chandrashekar, T. K. *J. Am. Chem. Soc.* **1983**, *105*, 4232.
(27) Makinen, M.; Mustafi, D. In *Metal Ions in Biological Systems*; Sigel, H., Sigel, A., Eds.; Marcel Dekker: New York, 1995; Vol. 31; p 89.
(28) Mustafi, D.; Makinen, M. W. *Inorg. Chem.* **1988**, *27*, 3360.
(29) Gerfen, G. J.; Hanna, P. A.; Chasteen, N. D.; Singel, D. J. *J. Am. Chem. Soc.* **1991**, *113*, 9513.
(30) Chasteen, N. D.; Belford, R. L.; Paul, I. C. *Inorg. Chem.* **1969**, *8*, 408.
(31) Francavilla, J.; Chasteen, N. D. *Inorg. Chem.* **1975**, *14*, 2860.
(32) LoBrutto, R.; Hamstra, B. J.; Colpas, G. J.; Pecoraro, V. L.; Frasch, W. D. *J. Am. Chem. Soc.* **1998**, *120*, 4410.
(33) Chen, W.; LoBrutto, R.; Frasch, W. D. *J. Biol. Chem.* **1999**, *274*, 7089.
(34) Albanese, N. F.; Chasteen, N. D. *J. Phys. Chem.* **1978**, *82*, 910.
(35) Velde, G. T.; Baerends, E. J. *J. Comput. Phys.* **1992**, *99*, 84.
(36) Versluis, L.; Ziegler, T. *J. Chem. Phys.* **1988**, *88*, 322.
(37) Schreckenbach, G.; Li, J.; Ziegler, T. *Int. J. Quantum Chem. Symp.* **1995**, *56*, 477.
(38) Stein, M.; van Lenthe, E.; Baerends, E. J.; Lubitz, W. *J. Phys. Chem. A* **2001**, *105*, 416.
(39) Belanzoni, P.; Baerends, E. J.; Gribnau, M. *J. Phys. Chem. A* **1999**, *103*, 3732.
(40) van Lenthe, E.; Baerends, E. J.; Snijders, J. G. *J. Chem. Phys.* **1993**, *99*, 4597.
(41) van Lenthe, E.; Baerends, E. J.; Snijders, J. G. *J. Chem. Phys.* **1994**, *101*, 9783.
(42) van Lenthe, E.; Snijders, J. G.; Baerends, E. J. *J. Chem. Phys.* **1996**, *105*, 6505.
(43) van Lenthe, E.; Leeuwen, R. v.; Baerends, E. J.; Snijders, J. G. *Int. J. Quantum Chem.* **1996**, *57*, 281.

(44) van Lenthe, E.; Ehlers, A. E.; Baerends, E. J. *J. Chem. Phys.* **1999**, *110*, 8943.
(45) Vosko, S. H.; Wilk, L.; Nusair, M. *Can. J. Phys.* **1980**, *58*, 1200.
(46) Becke, A. D. *Phys. Rev. A* **1988**, *38*, 3098.
(47) Perdew, J. P. *Phys. Rev. B* **1986**, *33*, 8822.
(48) Balhausen, C. J.; Djurinskij, B. F.; Watson, K. J. *J. Am. Chem. Soc.* **1968**, *90*, 3305.
(49) Martini, G.; Ottaviani, M. F.; Seravalli, G. L. *J. Phys. Chem.* **1975**, *79*, 9, 1716.
(50) Atherton, N. M.; Shakleton, J. F. *Chem. Phys. Lett.* **1984**, *103*, 302.
(51) Balhausen, C. J.; Gray, H. B. *Inorg. Chem.* **1962**, *1*, 111.
(52) van Willigen, H.; Mulks, C. F.; Atherton, N. M. *Inorg. Chem.* **1982**, *21*, 1708.
(53) Dikanov, S. A.; Yudanov, V. F.; Tsvetkov, Y. D. *J. Magn. Reson.* **1979**, *34*, 631.
(54) Alternatively, the data in Figure 2 could be fit to the functional form $A_{iso} = A + B \sin^2 \beta$, where A and B are equal to -1.79 and 12.86 MHz, respectively.
(55) Griller, D.; Ingold, K. U. *J. Am. Chem. Soc.* **1974**, *96*, 6715.
(56) Smith, T. S., II; Root, C. A.; Kampf, J. W.; Rasmussen, P. G.; Pecoraro, V. L. *J. Am. Chem. Soc.* **2000**, *122*, 767.
(57) Petersen, J.; Hawkes, T. R.; Lowe, D. J. *J. Am. Chem. Soc.* **1998**, *120*, 10978.
(58) Petersen, J.; Hawkes, T. R.; Lowe, D. J. *J. Inorg. Biochem.* **2000**, *80*, 161.
(59) Hamstra, B. J.; Houseman, A. L. P.; Colpas, G. J.; Kampf, J. W.; LoBrottu, R.; Frasch, W. D.; Pecoraro, V. L. *Inorg. Chem.* **1997**, *36*, 4866.
(60) Grant, C. V.; Geiser-Bush, K. M.; Cornman, C. R.; Britt, R. D. *Inorg. Chem.* **1999**, *38*, 6285.